# Ladder Structures in Lithium Amide Chemistry: Syntheses and Solid-State and Solution Structures of Donor-Deficient Lithium Pyrrolidide Complexes, $\{[H_2\overline{C(CH_2)_3NLi}]_3\cdot PMDETA\}_2$ and $\{[H_2\overline{C(CH_2)_3NLi}]_2\cdot TMEDA\}_2$, and ab Initio MO Calculations Probing Ring vs Ladder vs Stack Structural Preferences

**David R. Armstrong,[†] Donald Barr,[‡] William Clegg,[§] Susan M. Hodgson,[§] Robert E. Mulvey,[†] David Reed,[⊥] Ronald Snaith,*[,‡] and Dominic S. Wright[‡]**

*Contribution from the Departments of Chemistry, University of Strathclyde, Glasgow, G1 1XL, U.K., University of Cambridge, Cambridge, CB2 1EW, U.K., University of Newcastle upon Tyne, Newcastle upon Tyne, NE1 7RU, U.K., and University of Edinburgh, Edinburgh, EH9 3JJ, U.K.*
*Received August 4, 1988*

**Abstract:** Two donor-deficient lithium pyrrolidide complexes, $\{[H_2\overline{C(CH_2)_3NLi}]_3\cdot PMDETA\}_2$ (**1**) [PMDETA = $MeN(CH_2CH_2NMe_2)_2$] and $\{[H_2\overline{C(CH_2)_3NLi}]_2\cdot TMEDA\}_2$ (**2**) [TMEDA = $Me_2N(CH_2CH_2)NMe_2$], have been synthesized and characterized. X-ray diffraction has shown that both are dimers, each with central ladder arrangements consisting of two attached $(NLi)_2$ rings; in **1**, two terminal NLi·PMDETA units are partially broken off from the ladder, while in **2** the ladder is intact, its two end Li centers each being coordinated by a bidentate TMEDA ligand. Within these ladders the pyrrolidido N–Li distances around the central $N_2Li_2$ rings average 2.035 Å for **1** and 2.036 Å for **2**, while those of the (uncomplexed) ladder edges of the outer rings are shorter, averaging 1.950 and 1.963 Å, respectively; such values are interpreted in terms of ladder formation occurring from two isolated $(NLi)_2$ rings (with two-center N–Li bonds), these joining by formation of three-center (so longer) $N–Li_2$ bonds around the resulting inner $(NLi)_2$ ring. Ab initio calculations on models of $(LiNH_2)_4$ (6-31G basis set) and of complexed $(LiNH_2)_4\cdot 2H_2O$ and $(LiNH_2)_4\cdot 4H_2O$ species (STO-3G) have been used to probe the structural options of eight-membered ring vs ladder of two $(LiNH_2)_2$ dimeric rings vs stack (pseudocubane) of two such rings. For uncomplexed $(LiNH_2)_4$, the ring is found to be most stable, then the ladder (+7.4 kcal $mol^{-1}$), and then the stack (+11.4 kcal $mol^{-1}$). However, the ring-ladder order is reversed upon bis(complexation), $(LiNH_2)_4\cdot 2H_2O$ as a ladder (with an $H_2O$ ligand on each of the end-Li centers) being 7.2 kcal $mol^{-1}$ more stable than the same species as a ring (with an $H_2O$ ligand on two diagonally opposite Li centers). Further complexation, to give $(LiNH_2)_4\cdot 4H_2O$, intensifies this preference, a ladder model with each end Li bis(complexed) being 17.1 kcal $mol^{-1}$ lower in energy than a symmetrically solvated ring. However, a ladder model with an $H_2O$ ligand on each of the Li atoms (i.e., including the central ring ones) is considerably (by 62.9 kcal $mol^{-1}$) destabilized. These results tally therefore with the isolation of **1** and **2** as donor-deficient, purely end Li-complexed species, with ladder rather than ring structures. The solution structures of **1** and **2** were examined by variable-concentration cryoscopy in benzene solutions and by variable-temperature and -concentration $^6Li$, $^7Li$ NMR spectroscopic studies in $[^2H_8]$-toluene. While the results indicate that complex **2** largely retains its dimeric ladder structure in solution, for complex **1** relative molecular mass (so association state) values first increase but then decrease on concentration, and this is matched by the $^7Li$ NMR spectra of solutions first becoming more complex but then simplifying as concentration increases. The suggested explanation of such results is that, in dilute solutions, the role of the PMDETA within each ladder is amended to, for example, a bidentate mode; this would allow several such ladders to join together, though, in more concentrated solutions, such ligand amendment is suppressed and hence so too is further association.

Lithium amides (amidolithiums), RR′NLi, are widely used reagents in organometallic and organic syntheses; in the former, their reaction with M–X bonds (e.g., X = Hal, OR″) leads to LiX elimination and amide group transfer giving M–NRR′ products,[1] while in the latter they are employed as efficient proton abstraction agents, often with high regio- and stereoselectivity.[2] Until quite recently, solutions of such reagents were generally prepared in situ by lithiation of amines and then used forthwith in subsequent reactions of the types just described. However, as pointed out in 1983,[3] there are obvious advantages in first isolating such materials: most importantly, to guarantee reagent purity and to permit weighing out of stoichiometric amounts for further reaction (rather than assuming a 100% yield from the amine lithiation). More fundamentally than these considerations, however, is that such isolation permits proper identification, in the fullest sense, of the lithium amide.[4] To elaborate, firstly "RR′NLi" is a misnomer since, as we show below, such species would be either oligomers, $(RR'NLi)_n$, $n$ = 3, 4, of limited solubility or, more usually, polymeric materials, insoluble in hydrocarbon media: it is for precisely this reason that most such reagents need to be made in the presence of Lewis base (L) solvents, so that they are in fact *complexes* of form $(RR'NLi\cdot xL)_n$. Secondly, from this, in order to begin to understand exactly how these reagents then operate, the value(s) of $x$ and of $n$ must be established in the solid state and, even more importantly, in solution.

Through the work of many groups (perhaps most notably those of Dietrich, Oliver, Schleyer, Streitwieser, and Weiss) it is now well-recognized that most oligomeric organic lithium compounds

* Address correspondence to the following address: University Chemical Laboratory, Lensfield Road, Cambridge, CB2 1EW, U.K.
† University of Strathclyde.
‡ University of Cambridge.
§ University of Newcastle upon Tyne.
⊥ University of Edinburgh.

(1) Lappert, M. F.; Power, P. P.; Sanger, A. R.; Srivastava, R. C. *Metal and Metalloid Amides*; Wiley: New York, 1980.
(2) (a) Stowell, J. C. *Carbanions in Organic Synthesis*; Wiley-Interscience: New York, 1979. (b) Fieser, M. *Fieser's Reagents for Organic Synthesis*; Wiley-Interscience: New York, 1986; Vol. 12 and earlier volumes give specific uses of lithium amides arranged according to individual Li–N compounds.
(3) Lappert, M. F.; Slade, M. J.; Singh, A.; Atwood, J. L.; Rogers, R. D.; Shakir, R. *J. Am. Chem.Soc.* **1983**, *105*, 302.
(4) Armstrong, D. R.; Mulvey, R. E.; Walker, G. T.; Barr, D.; Snaith, R. *J. Chem. Soc., Dalton Trans.* **1988**, 617.

0002-7863/89/1511-4719$01.50/0 

**Scheme I**

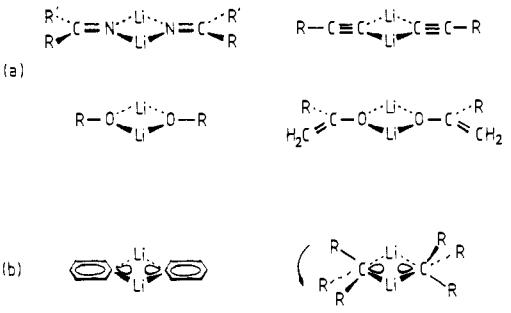

**Scheme II**

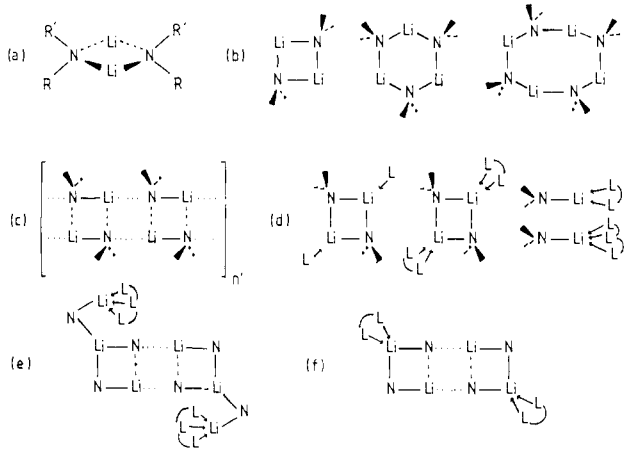

have cluster structures, commonly hexameric and tetrameric ones.[5] We have recently put forward a rationalization of such clustering behavior in terms of ring-stacking ideas.[6]

Thus, for species such as iminolithiums $(RR'C{=}NLi)_n$, alkynyllithiums $(RC{\equiv}CLi)_n$, alkoxy- and aryloxylithiums $(ROLi)_n$, and enolatolithiums $[R(=CH_2)COLi]_n$, the basic unit is a four- or six-membered ring of Li and X atoms (X = N, C, O, and O, respectively): as Scheme Ia illustrates, the crucial feature is that such ring systems are flat up to and including (at least) the primary atom of the group(s), R, and hence they can associate vertically ("stack") giving oligomeric clusters with, typically, $n = 6$ or 4 (double stacks of trimeric or dimeric rings) or polymers with $n = \infty$ (continuous stacks). Similar structural preferences are found for aryl- and alkyllithiums [Scheme Ib] since in the former the aryl group can be coplanar with the $(CLi)_{2,3}$ ring and in the latter the R groups can rotate to allow interlocking of $(CLi)_{2,3}$ rings: both situations can occur without detriment to the $C{-}Li_2$ ring bonding, since each C atom presents just one lobe into the ring. Crucially, though, these structural options based on vertical associations of rings do not exist for lithium amides. Thus, as depicted in Scheme IIa, outside a planar $(NLi)_n$ ring system (shown for $n = 2$, but also available with $n = 3$ or 4) the $sp^3$ nature of the amido N atoms causes the R,R′ groups to be projected above and below such a ring, so precluding stacking: hence, despite their just noted preponderance elsewhere in organolithium chemistry, no clustered amidolithiums (e.g., hexamers or cubane-like tetramers) are known experimentally. Instead, these oligomeric $(RR'NLi)_n$ rings themselves are isolated as such [$n = 2$, 3, 4; Scheme IIb], or seemingly polymeric materials result. Concerning the polymers, continuous ring association must presumably have taken place *laterally*, joining (NLi) ring edges [cf. $(NLi)_{2,3}$ ring faces in the case of stacks] and so giving ladders[7] or fences[8] [Scheme IIc] in which central Li atoms have increased their coordination number from 2 in the constituent rings to 3. Although such extended ladders will be amorphous materials, unlikely to be amenable to X-ray structural investigation, treatment with Lewis base donors (L) will lead to crystalline oligomers. Where a 1:1 Li:L ratio is available, constituent dimeric rings or (monomeric) N–Li edges will result, depending on the denticity of the donor and the sizes of L and R,R′ groups; complexes typified in Scheme IId are thus isolated. However, it should be possible to retain *limited* ladder structures [e.g., Scheme IIe and f] by provision of a *deficiency* of donor: confirmation of this would provide at least indirect evidence that association of $(RR'NLi)_n$ rings to give polymers does indeed occur by a continuation of such laddering.

This paper describes the first isolation of such intercepted lithium amide ladders. It concentrates on (i) the syntheses, characterizations, and X-ray structures of two complexed pyrrolididolithium ladders [pyrrolidido = $H_2\overline{C(CH_2)_3N}$-], $\{[H_2\overline{C(CH_2)_3NLi}]_3{\cdot}PMDETA\}_2$ (**1**) (reported in a preliminary communication[7]), PMDETA = $MeN(CH_2CH_2NMe_2)_2$, and $\{[H_2\overline{C(CH_2)_3NLi}]_2{\cdot}TMEDA\}_2$ (**2**), TMEDA = $Me_2N(CH_2)_2NMe_2$; (ii) ab initio MO calculations on the structural options, ring vs ladder vs stack, available to such lithium amide species; and (iii) the behavior of these donor-deficient lithium amide complexes in hydrocarbon solutions (the media in which they could be used in organic syntheses), as elucidated by cryoscopic and high field $^{6,7}Li$ NMR spectroscopic studies at various concentrations and temperatures.

## Experimental Section

**General Procedures.** Standard inert atmosphere techniques were used for the preparations and subsequent investigations of the compounds described. For analyses, C, H, and N values were determined by using a Perkin-Elmer 240 elemental analyzer and Li by using a 360 Perkin-Elmer atomic absorption spectrometer. High field NMR spectra were recorded on a Bruker WH 360-MHz NMR spectrometer operating at 360.13 MHz for $^1H$ {in [$^2H_6$]benzene solutions, proton chemical shifts being given relative to external $SiMe_4$; all shifts are positive to high frequency of standards} and at 139.96 MHz for $^7Li$, [$^2H_8$]toluene solutions being externally referenced to the $^7Li$ signal of phenyllithium in the same solvent ($\Xi$ value, 38.863 882 MHz). Selected $^6Li$ NMR spectra were also recorded on the same spectrometer, at 52.99 MHz, with [$^2H_8$]toluene solutions externally referenced to $Ph^6Li$ in the same solvent ($\Xi$ value, 14.716 115 MHz). Such $^6Li$ NMR spectra were obtained using 30° pulses and pulse repetition times of ca. 1 s.

Cryoscopic relative molecular mass (CRMM) measurements on variable-concentration benzene solutions of **1** and **2** were carried out as previously described.[9]

**Synthesis of $[H_2\overline{C(CH_2)_3NLi}]_n$.** A solution of pyrrolidine, $H_2\overline{C(CH_2)_3NH}$ (10 mmol, 0.71 g), in hexane (5 mL) was chilled, and butyllithium (10 mmol, 5.9 mL of a 1.7 mol $dm^{-3}$ solution in hexane) was slowly added to it. On warming to room temperature, a white precipitate was produced: this was filtered off, washed with hexane, and identified as pyrrolididolithium, $[H_2\overline{C(CH_2)_3NLi}]_n$: yield, 0.73 g, 95%; mp dec 150 °C. Anal. Calcd for $C_4H_8LiN$: C, 62.3; H, 10.4; Li, 9.1; N, 18.2. Found: C, 62.1; H, 10.4; Li, 9.0; N, 18.0. The compound was insoluble

(5) (a) For reviews and accounts of the structural features of organic lithium compounds, see: Oliver, J. P. *Adv. Organomet. Chem.* **1977**, *15*, 235. Wardell, J. L. *Comprehensive Organometallic Chemistry*; Wilkinson, G., Stone, G. A., Abel, E. W., Eds.; Pergamon: Oxford, 1982; Vol. 1, p 43. Schleyer, P. v. R. *Pure Appl. Chem.* **1983**, *55*, 355; **1984**, *56*, 151. Setzer, W.; Schleyer, P. v. R. *Adv. Organomet. Chem.* **1985**, *24*, 353. (b) For some specific crystal structures of tetramers and hexamers, see: Dietrich, H. *Acta Crystallogr.* **1963**, *168*, 681; *J. Organomet. Chem.* **1981**, *205*, 291 [$(EtLi)_4$ structure]. Weiss, E.; Lucken, E. A. C. *J. Organomet. Chem.* **1964**, *2*, 197. Weiss, E.; Hencken, G. *J. Organomet. Chem.* **1970**, *21*, 265 [$(MeLi)_4$ structure]. Tecle', B.; Rahman, A. F. M. M.; Oliver, J. P. *J. Organomet. Chem.* **1986**, *317*, 267 [$(Me_2SiCH_2Li)_6$ structure]. (c) For typical theoretical MO calculations on organolithium species see the following and references therein: Streitwieser, A. *Acc. Chem. Res.* **1984**, *17*, 353. Bachrach, S. M.; Streitwieser, A. *J. Am. Chem. Soc.* **1984**, *106*, 2283. Rajca, A.; Streitwieser, A.; Tolbert, L. M. *J. Am. Chem. Soc.* **1987**, *109*, 1790.

(6) (a) Barr, D.; Clegg, W.; Mulvey, R. E.; Snaith, R.; Wade, K. *J. Chem. Soc., Chem. Commun.* **1986**, 295. (b) Armstrong, D. R.; Barr, D.; Snaith, R.; Clegg, W.; Mulvey, R. E.; Wade, K.; Reed, D. *J. Chem. Soc., Dalton Trans.* **1987**, 1071. (c) Barr, D.; Snaith, R.; Clegg, W.; Mulvey, R. E.; Wade, K. *J. Chem. Soc., Dalton Trans.* **1987**, 2141.

(7) Armstrong, D. R.; Barr, D.; Clegg, W.; Mulvey, R. E.; Reed, D.; Snaith, R.; Wade, K. *J. Chem. Soc., Chem. Commun.* **1986**, 869.

(8) Kato, H.; Hirao, K.; Akagi, K. *Inorg. Chem.* **1981**, *20*, 3659.

(9) Reed, D.; Barr, D.; Mulvey, R. E.; Snaith, R. *J. Chem. Soc., Dalton Trans.* **1986**, 557.

in aromatic solvents, precluding $^1H$ and $^{13}C$ NMR studies.

**Synthesis of $\{[H_2C(CH_2)_3NLi]_3 \cdot PMDETA\}_n$, 1.** Pyrrolidine (10 mmol, 0.71 g) was added to a frozen solution of Bu$^n$Li (10 mmol, 5.9 mL of a 1.7 mol dm$^{-3}$ solution in hexane) and PMDETA (10 mmol, 1.73 g). A white precipitate appeared on warming to room temperature, subsequent addition of hot toluene (4 mL) causing dissolution to a pale yellow solution. Slow cooling gave large pale yellow needles identified as complex **1**: yield, 1.20 g, 89%; mp 118–120 °C; $^1H$ NMR multiplet centered at $\delta$ 3.30 ppm [12 H; 3 × $(CH_2)_2$ of three pyrrolidido ligands; cf. m, centered $\delta$ 2.73 in pyrrolidine], overlapping multiplets $\delta$ 2.30–1.70 ppm [35 H; 3 × $(CH_2)_2$ of three pyrrolidido ligands, 2 × $NMe_2$ + NMe + 2 × $(CH_2)_2$ of one PMDETA ligand; cf. m, centered $\delta$ 1.50 in pyrrolidine, s (3 H), $\delta$ 2.20, s (12 H) $\delta$ 2.14, and s (8 H) $\delta$ 2.43 in PMDETA]. Anal. Calcd for $C_{21}H_{47}Li_3N_6$: C, 62.4; H, 11.6; Li, 5.2; N, 20.8. Found: C, 61.5; H, 11.4; Li, 4.9; N, 19.7.

**Synthesis of $\{[H_2C(CH_2)_3NLi]_2 \cdot TMEDA\}_n$, 2.** Addition of Bu$^n$Li (10 mmol, 5.9 mL of a 1.7 mol dm$^{-3}$ solution in hexane) to a frozen solution of pyrrolidine (10 mmol, 0.71 g) and TMEDA (10 mmol, 1.16 g) in hexane (5 mL), followed by warming to room temperature, produced a colorless solution. Chilling at −10 °C gave colorless, parallelopiped crystals of complex **2**: yield of first batch, 1.08 g, 80%; mp 129–130 °C; $^1H$ NMR multiplet centered at $\delta$ 3.02 ppm [8 H; 2 × $(CH_2)_2$ of two pyrrolidido ligands], multiplet centered at $\delta$ 1.60 ppm [8 H; 2 × $(CH_2)_2$ of two pyrrolidido ligands], s, $\delta$ 1.95 ppm (12 H; 2 × $NMe_2$ of one TMEDA ligand; cf. s, $\delta$ 2.13 in TMEDA), s, $\delta$ 1.86 ppm [4 H, $(CH_2)_2$ of one TMEDA ligand; cf. s, $\delta$ 2.33 in TMEDA]. Anal. Calcd for $C_{14}H_{32}Li_2N_4$: C, 62.2; H, 11.9; Li, 5.2; N, 20.7. Found: C, 61.1; H, 11.9; Li, 5.2; N, 20.4.

**X-ray Crystallography.** Crystals of complexes **1** and **2** suitable for X-ray analysis were transferred in a nitrogen-filled glovebox to Lindemann glass capillary tubes which were then sealed prior to data collection. This was performed at room temperature (22 °C) on a Siemens AED2 diffractometer with graphite-monochromated Cu K$\alpha$ radiation ($\lambda$ = 1.541 84 Å), $\omega/\theta$ scans, and an on-line profile-fitting technique.[10] Cell parameters were refined from $2\theta$ values of reflections measured at $\pm\omega$. No absorption corrections were applied. Atomic scattering factors were taken from ref 11. The structures were solved by direct methods and refined on $F$ by blocked-cascade least squares[12] with the weighting scheme $w^{-1} = \sigma^2(F) = \sigma^2_c(F) + A_1 + A_2G + A_3G^2 + A_4S + A_5S^2 + A_6GS$, where $\sigma_c(F)$ is based on counting statistics alone, $G = F_o/F_{max}$, $S = \sin\theta/\sin\theta_{max}$, and the $A_n$ parameters are derived empirically by an optimization of the variance of analysis.[13] Further details are given in Table I.

**MO Calculations.** The ab initio-derived optimized geometries described were obtained from the computer program GAMESS[14] using the 6-31G basis set[15] and the STO-3G basis set.[16]

## Results and Discussion

Lithiation of pyrrolidine in hexane alone proceeds quantitatively to give a white, amorphous, and hydrocarbon-insoluble material, pyrrolididolithium, $[H_2C(CH_2)_3NLi]_n$; this we believe to be a polymeric ladder of the kind shown in Scheme IIc. Such continuous association is particularly favored when the R,R′ groups of $(RR'NLi)_n$ are small and/or flat, e.g., $[Ph(Me)NLi]_n$ and $(Ph_2NLi)_n$ are also polymeric,[17] and yet more so when they are tied together, as in the pyrrolidide ligand. Significantly, it is only when such groups are bulky and/or "floppy" [so using up lateral

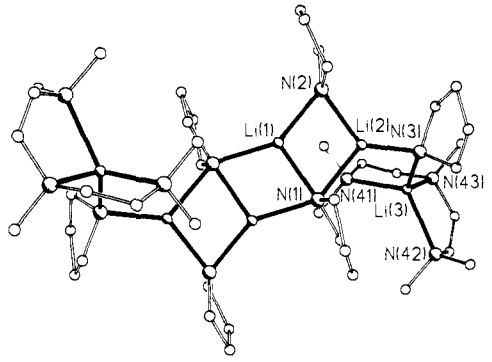


**Figure 1.** Molecular structure of **1**, with the labeling scheme for Li and N atoms and without H atoms. Li–N bonds are drawn thicker.

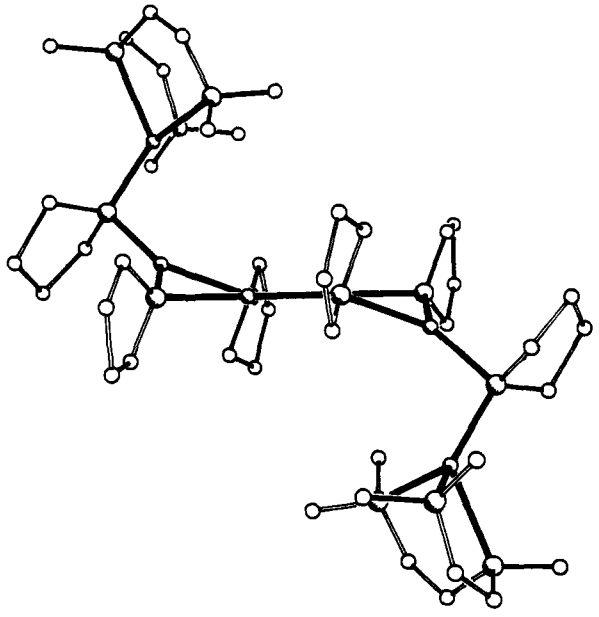

**Figure 2.** The structure of **1** seen edge on to the central $Li_2N_2$ ring.

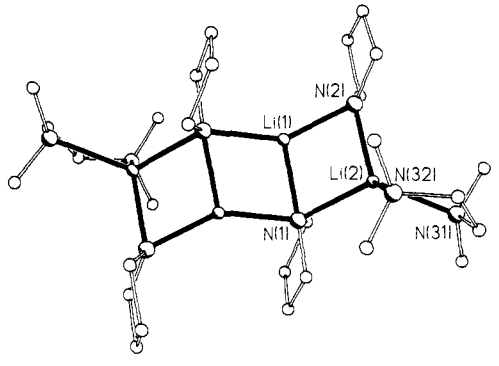


**Figure 3.** Molecular structure of **2**, drawn as for **1** in Figure 1.

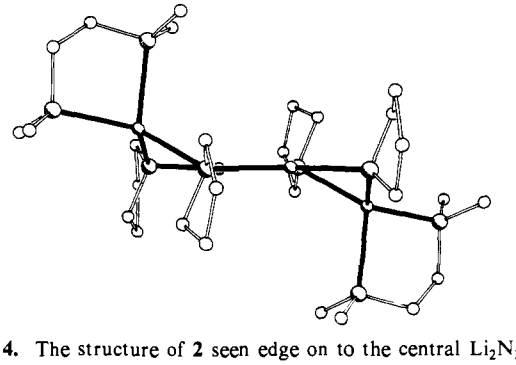

**Figure 4.** The structure of **2** seen edge on to the central $Li_2N_2$ ring.

(10) Clegg, W. *Acta Crystallogr., Sect. A* **1981**, *37*, 22.
(11) *International Tables for X-ray Crystallography*; Kynoch Press: Birmingham, U.K., 1974; Vol. 4, pp 99, 149.
(12) Sheldrick, G. M. SHELXTL, an integrated system for solving, refining, and displaying crystal structures from diffraction data, Revision 5, University of Göttingen: Federal Republic of Germany, 1985.
(13) Hong, W.; Robertson, B. E. *Structure and Statistics in Crystallography*; Wilson, A. J. C., Ed.; Adenine: New York, 1985; p 125.
(14) (a) Dupuis, M.; Spangler, D.; Wendoloski, J. J. GAMESS, N.R.C.C. Software Catalogue, Program No. 2 GOI, 1980; Vol. 1. (b) Guest, M. F.; Kendrick, J.; Pope, S. A. GAMESS Documentation, Daresbury Laboratory, 1983.
(15) (a) Hehre, W. J.; Ditchfield, R.; Pople, J. A. *J. Chem. Phys.* **1972**, *56*, 2257. (b) Hariharan, P. C.; Pople, J. A. *Theor. Chim. Acta* **1973**, *28*, 213. (c) Dill, J. D.; Pople, J. A. *J. Chem. Phys.* **1975**, *62*, 2921.
(16) (a) Hehre, W. J.; Stewart, R. F.; Pople, J. A. *J. Chem. Phys.* **1969**, *51*, 2657. (b) Hehre, W. J.; Ditchfield, R.; Stewart, R. F.; Pople, J. A. *J. Chem. Phys.* **1970**, *52*, 2769.
(17) Barr, D.; Clegg, W.; Mulvey, R. E.; Snaith, R.; Wright, D. S. *J. Chem. Soc., Chem. Commun.* **1987**, 716.

**Table I.** Crystallographic Data

| | 1 | 2 |
|---|---|---|
| formula | $C_{42}H_{94}Li_6N_{12}$ | $C_{28}H_{64}Li_4N_8$ |
| form wt | 808.9 | 540.6 |
| cryst syst | monoclinic | monoclinic |
| space gp | $C2/c$ | $P2_1/n$ |
| $a$, Å | 20.746 (2) | 10.423 (1) |
| $b$, Å | 16.927 (2) | 12.559 (1) |
| $c$, Å | 17.695 (2) | 14.032 (1) |
| $\beta$, deg | 119.00 (1) | 95.75 (1) |
| $V$, Å$^3$ | 5434.8 | 1827.6 |
| $Z$ | 4 | 2 |
| $d_{calcd}$, g cm$^{-3}$ | 0.988 | 0.982 |
| $F(000)$ | 1792 | 600 |
| $\mu$(Cu K$\alpha$), mm$^{-1}$ | 0.41 | 0.41 |
| cryst size, mm | 0.21 × 0.21 × 0.77 | 0.35 × 0.35 × 0.80 |
| $2\theta_{max}$, deg | 130 | 130 |
| reflcns measd | 5463 | 5458 |
| unique reflcns | 4549 | 2988 |
| reflcns with $F > 4\sigma_c(F)$ | 2057 | 2324 |
| $R_{int}$ | 0.025 | 0.015 |
| no. params | 272 | 182 |
| weighting params $A$ | 17, 157, −110, −41, 32, −277 | 16, −78, 89, −385, 22, 111 |
| $R$ | 0.091 | 0.083 |
| $wR$ | 0.094 | 0.052 |
| max, mean shift/esd | 0.015, 0.003 | 0.010, 0.003 |
| $S$ | 1.05 | 1.48 |
| max, min in diff map, e Å$^{-3}$ | 0.29, −0.17 | 0.39, −0.24 |

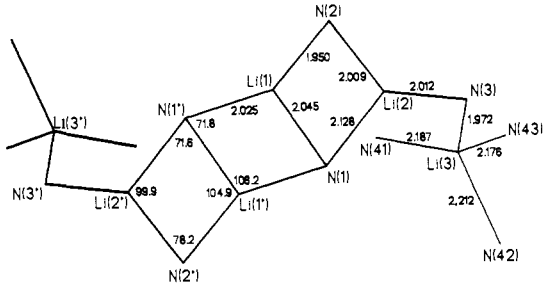


**Figure 5.** Li–N bond lengths and ring internal angles for **1**. Esd values are in the range 0.008–0.013 Å and 0.4–0.6°.

space around the $(NLi)_n$ ring] that ring oligomers of the type shown in Scheme IIb can be isolated: $n = 2$ for $[(Me_3Si)_2NLi]_2$ (but only in the gas phase),[18] $n = 3$ for crystalline $[(Me_3Si)_2NLi]_3$[19] and $[(PhCH_2)_2NLi]_3$,[4,20] and $n = 4$ for $[Me_2\overline{C(CH_2)_3CMe_2NLi}]_4$.[3]

When pyrrolidine is lithiated in the additional presence of the Lewis base (L) donors PMDETA and TMEDA (amine:Bu$^n$Li:L ratio, 1:1:1), crystalline, hydrocarbon-soluble complexes **1** and **2** result, respectively. The same products are formed, in similarly high yields, when reactants are brought together in proper stoichiometric amounts according to the formulas of **1** and **2**, i.e., amine:Bu$^n$Li:L ratio of 3:3:1 and of 2:2:1, respectively. Both complexes were fully characterized by elemental analyses and by their $^1$H NMR spectra which established conclusively their pyrrolidide:L ratios. In addition, their IR spectra contained absorptions typical of L and of pyrrolidine, though with no $\nu$(NH) band (cf. in pyrrolidine itself, at 3278 cm$^{-1}$); such amine bands, and ones due to LiOH [$\nu$(OH), 3680 cm$^{-1}$), appeared on the briefest air exposure of these Nujol mulls.

The crystal structures of **1** and **2** have been determined. Two views of each molecule are given, in Figures 1 and 2 for **1** and in Figures 3 and 4 for **2**. In addition, Figures 5 and 6 show important bond lengths and angles for **1** and **2**, respectively; full tables of bond distances and angles constitute part of the Supplementary Material. The structure of **1** (Figure 1) consists of a central ladder-type arrangement of two attached $(NLi)_2$ rings (or, alternatively, four amido N–Li rungs) with, partially broken off from this, two terminal N–Li units each complexed by PMDETA [cf. Scheme IIe]; the continuous intact ladder envisaged for $[H_2\overline{C(CH_2)_3NLi}]_n$ has thus been intercepted by these donors but, in doing so, it has also been partly fragmented. The central ring of the ladder, $\overline{N(1)Li(1)\cdot N(1')Li(1')}$, is strictly planar, and the N atoms of the outer rungs [N(2), N(2′)] are essentially in this same plane (within 0.006 Å). However, as shown in a side-view of the structure of **1** (Figure 2), the corresponding Li atoms [Li(2),Li(2′)] deviate from this common plane by ±0.71 Å, presumably due to the steric effects of the terminal N–Li·PMDETA groups. The structure of complex **2** shows very similar features (Figure 3), though now, containing a bidentate (TMEDA) donor, there is no fragmentation [cf. Scheme IIf]: the central ring, $\overline{N(1)Li(1)\cdot N(1')Li(1')}$, is planar, with the N atoms of the outer rungs [N(2),N(2′)] lying also near this plane (within 0.102 Å) but with the end-Li atoms [Li(2),Li(2′)] displaced from it by ±1.01 Å (Figure 4). Similar intact ladder structures have also been observed for the lithium diorganophosphides $[Li_2(\mu_3\text{-}Bu^t{}_2P)(\mu_2\text{-}Bu^t{}_2P)\cdot THF]_2$[21] and $\{Li_2[\mu_3\text{-}(Me_3Si)_2P]\cdot[\mu_2\text{-}(Me_3Si)_2P]\cdot THF\}_2$,[22] though here, due to the presence of monodentate donors and so three-coordinate end-Li atoms, the $Li_4P_4$ frameworks are essentially all-planar. A dimeric lithium enolate–lithium amide mixed-ladder species, $\{Li_2[\mu_3\text{-}OC(=CH_2)\cdot CMe_2(CH_2)_2\cdot OSiMe_2Bu^t](\mu_2\text{-}NPr^i{}_2)\}_2$ with central Li–O and end Li–N edges, has also been described recently.[23]

The dimensions within **1** and **2** merit attention (Figures 5 and 6, respectively). Firstly, the angles within the planar central rings $\overline{N(1)Li(1)\cdot N(1')Li(1')}$ average 108.2° at Li and 71.8° at N, and these seem little altered from the values expected for an uncomplexed $(RR'NLi)_2$ ring: none such are known in the solid state {though in the gas-phase structure of $[(Me_3Si)_2NLi]_2$ the angle at Li was ca. 100°}[18] but in dimeric complexes of form $(RR'NLi\cdot L)_2$ the angles at Li and at N are typified by those found for $[(PhCH_2)_2NLi\cdot OEt_2]_2$, 104.0° and 76.0°, respectively.[4] In the end rings, $\overline{N(1')Li(1')N(2')Li(2')}$ and $\overline{N(1)Li(1)N(2)Li(2)}$,

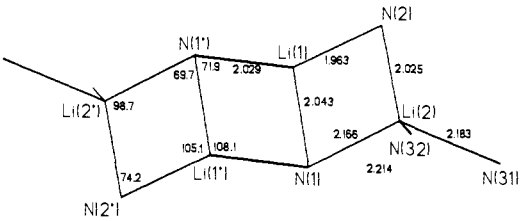


**Figure 6.** Li–N bond lengths and ring internal angles for **2**. Esd values are 0.005 Å and 0.2–0.3°.

**Scheme III**

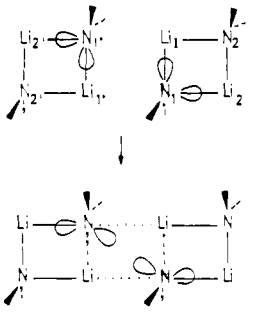

(18) Fjeldberg, T.; Hitchcock, P. B.; Lappert, M. F.; Thorne, A. J. *J. Chem. Soc., Chem. Commun.* **1984**, 822.
(19) Rogers, R. D.; Atwood, J. L.; Grüning, R. *J. Organomet. Chem.* **1978**, *157*, 229.
(20) Barr, D.; Clegg, W.; Mulvey, R. E.; Snaith, R. *J. Chem. Soc., Chem. Commun.* **1984**, 285, 287.
(21) Jones, R. A.; Stuart, A. L.; Wright, T. C. *J. Am. Chem. Soc.* **1983**, *105*, 7459.
(22) Hey, E.; Hitchcock, P. B.; Lappert, M. F.; Rai, A. K. *J. Organomet. Chem.* **1987**, *325*, 1.
(23) Williard, P. G.; Hintze, M. J. *J. Am. Chem. Soc.* **1987**, *109*, 5539.

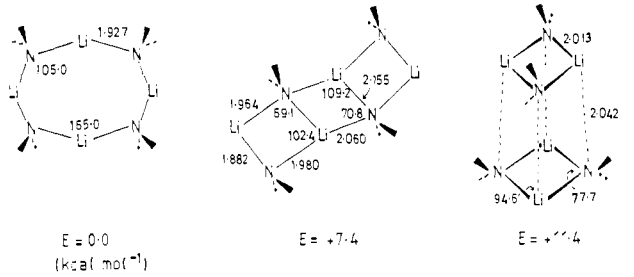


**Figure 7.** Ab initio optimized geometries (6-31G level) of $(LiNH_2)_4$ structures: planar ring ($D_{4h}$), ladder ($C_{2h}$), and stack ($D_{2d}$) models.

of **1** and **2**, however, there are considerable distortions of these angles: most notably, their sum is only 352.6° for **1** and 347.7° for **2**, and there is a wider angle at the inner Li atoms [Li(1),Li(1′), average 105.0°] than at the outer ones [Li(2),Li(2′), average 99.3°]. Turning to N–Li bond distances, those involving the Lewis base ligands are unremarkable, averaging 2.191 Å in **1** and 2.199 Å in **2** and so comparable with (PMDETA)N–Li and (TMEDA)N–Li distances of 2.21 and 2.296 Å within Ph(Naphthyl)NLi·PMDETA and $[Ph(Me)NLi\cdot TMEDA]_2$, respectively.[17] However, for the pyrrolidide N–Li distances, there is a clear pattern, and one intelligible in terms of the formation of a central ladder from two $(NLi)_2$ rings. As shown in Scheme III (which uses the same atom labels as Figures 1, 3, 5, and 6), in the isolated rings the N atoms each present two lobes [shown for N(1), N(1′)] for bonding to two Li centers: in total there are three electrons available from each RR′N ligand or two lone pairs if one considers the bonding to be essentially ionic, $RR'N^-$ to $Li^+$, but, either way, short, two-center N–Li bonds will result. However, for such rings to come together the electron density in these N lobes must be spread over three Li centers. This requires one of these lobes to engage in a 3-center $N–Li_2$ interaction involving an N–Li rung [an "intradimer" contact, e.g., N(1)···Li(1)] and a new N–Li edge [e.g., N(1)···Li(1′)] connecting the dimers: these bonding contacts are thus expected to be longer (not shorter, as asserted in ref 22) than the N–Li ladder edges emanating from the original dimers since these remain as essentially two-center two-electron bonds. Inspection of Figures 5 and 6 show that this is indeed the case, the lengths of the N–Li bonds around the central ring N(1)-Li(1)N(1′)Li(1′) averaging 2.035 Å for **1** and 2.036 Å for **2**, while the ladder edges of the outer rings [those unaffected by complexation with NLi·PMDETA or TMEDA, i.e., N(2)Li(1), N(2′)Li(1′)] have lengths of 1.950 Å for **1** and 1.963 Å for **2**.

To further probe the structural preferences of lithium amides and particularly to see how a ladder structure rates in such preferences, we have carried out ab initio MO calculations (6-31G basis set) on the uncomplexed tetramer $(LiNH_2)_4$ and on complexed versions of this, $(LiNH_2)_4\cdot 2H_2O$ and $(LiNH_2)_4\cdot 4H_2O$, at the lower level of STO-3G. Three alternative structures were considered for $(LiNH_2)_4$: a planar, eight-membered ring ($D_{4h}$), a cubane-like stack of two dimeric rings ($D_{2d}$), and a ladder formed by lateral association of two dimeric rings ($C_{2h}$). These three optimized structures are shown in Figure 7 which incorporates their key geometric features and notes their relative energies (kcal mol$^{-1}$). The only constraint applied to these optimizations was that needed to maintain symmetry; i.e., the ladder was kept planar and those parameters consistent with $C_{2h}$ were made equal. The ring and the cubane had been examined in an earlier study,[24] the former being found more stable by 11.5 (3-21G), 9.8 (6-31G calculation on the 3-21G optimized geometries); our value is 11.4 kcal mol$^{-1}$. However, we find the ladder-like structure to be a local minimum, intermediate in energy between the ring and the stack, and only 7.4 kcal mol$^{-1}$ higher in energy than the former. On electronegativity grounds alone, the bonding in these N–Li species must be largely ionic; however, when the calculations were repeated on $(Li^+\cdot NH_2^-)_4$, although the ring structure was again found to be the most stable, next in energy came the cubane (+0.9 kcal mol$^{-1}$) and then the ladder (a further 0.8 kcal mol$^{-1}$). A purely electrostatic treatment thus predicts not only a different order of stability but also a much closer, less differentiating, one: these observations presumably reflect at least a degree of covalent bonding/mutual anion–cation polarization in these species.

Closer inspection of $(LiNH_2)_4$ geometries allows one to rationalize these structural preferences. Thus, in the ring, the angles at Li (165.0°) and at N (105.0°) [cf. 168.5° and 101.5°, respectively, in the crystal structure of $[Me_2C(CH_2)_3CMe_2NLi]_4$[3]] and the N–Li distances of 1.927 Å lead to closest repulsive Li···Li and N···N contacts (two such, for each Li and each N atom) of 3.058 and 3.821 Å, respectively; the third, fully cross-ring distance for each Li is 4.325 Å and for each N is 5.403 Å. In contrast, the stack exhibits weaker N–Li bonding (distances being 2.013 Å within constituent rings, 2.042 Å between them) and much closer Li···Li and N···N contacts (for Li, 2.528 Å within each ring, two distances per Li of 2.343 Å between atoms in different rings; for N, the corresponding values are 2.960 and 3.297 Å). Linked to these points, in such a stack it is seen that the H atoms of the $NH_2$ ligands do indeed project essentially above and below the $(NLi)_2$ constituent rings [cf. Scheme IIa]: in practical systems $(RR'NLi)_n$, with $n = 4$ or higher and with R,R′ ≠ H, the steric demands of R,R′ groups should inhibit stacking even more. Two other sets of MO calculational results are relevant here. Firstly, ones on $(LiH)_4$ have shown that while an eight-membered ring is most stable, a stack of two dimeric rings (named as a "ring-dimer") comes next in energy (~3.7 kcal mol$^{-1}$ less stable), followed by a ladder (or "fence", 5.3 kcal mol$^{-1}$ less stable still):[8] this reversal of stack/ladder preference is readily intelligible since for $(LiH)_4$ there are of course *no* groups projecting from the $(LiH)_2$ constituent rings, so their close vertical approach would not be precluded.

Secondly, and more comparable with our own studies reported here, recent calculations on $(LiNH_2)_6$ hexamers predicted that a stacked structure of two trimers (distorted octahedral, $D_{3d}$) would be more stable (by 22.9 kcal mol$^{-1}$, 6-31G level) than a planar ring structure ($D_{6h}$):[25] once more, this is unsurprising since for $(LiX)_n$ rings in general there must come a point when, as $n$ increases, the ever-widening angles at Li and X make effective ring bonding unsustainable [indeed, in the above-mentioned $(LiH)_n$ calculations, a ring structure was most stable when $n = 5$, but not when $n = 6$]. However, the surprising aspect of this study of $(LiNH_2)_6$ species was that preliminary results implied that a ladder of six N–Li rungs (a "6 × 2 fence", $C_{2h}$) was intermediate in energy between the stack and the ring, i.e., less stable than the former. The validity and implications of these results have been discussed in detail elsewhere,[26] and suffice it to write here that we expect this apparent preference of $(LiNH_2)_6$ for a stack rather than a ladder to be reversed in real, experimental systems: the perpendicular orientations of R,R′ groups (with R,R′ ≠ H) will preclude stacking (even more so when it is attempted to stack more than two rings), and such steric inhibition will be intensified when the Li atoms in these rings bear Lewis base donors (whose presence will anyway, as discussed earlier, be needed if oligomeric species, rather than polymers, are to be isolated). One can add the (admittedly transient) experimental evidence that $(RR'NLi)_n$ rings are known, as now are ladders, but there are no known lithium amide stacked structures.

Returning to the intermediate energy ladder structure of $(LiNH_2)_4$, Figure 7, analysis of its dimensions allows rationalization of this intermediacy. Thus, the N–Li bond lengths range from 1.882 Å (the end rungs) to 2.155 Å (the inner rungs), and they average 1.995 Å around the outer rings, 2.108 Å around the inner one, and 2.008 Å over all ten N–Li bonds (cf. 1.927 Å for all eight bonds in the ring structure and an average of 2.023 Å

(24) Sapse, A.-M.; Raghavachari, K.; Schleyer, P. v. R.; Kaufmann, E. *J. Am. Chem. Soc.* **1985**, *107*, 6483.

(25) Raghavachari, K.; Sapse, A.-M.; Jain, D. C. *Inorg. Chem.* **1987**, *26*, 2585.

(26) For comments on the contents of ref 25, see: Clegg, W.; Snaith, R.; Wade, K. *Inorg. Chem.* **1988**, *27*, 3861. For a response to these comments, see: Raghavachari, K.; Sapse, A.-M.; Jain, D. C. *Inorg. Chem.* **1988**, *27*, 3862.

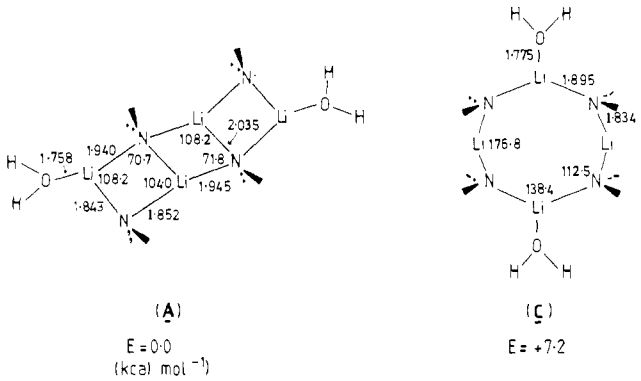


Figure 8. Ab initio optimized geometries (STO-3G) of $(LiNH_2)_4 \cdot 2H_2O$: (A) ladder model, with $H_2O$ molecules on outer Li atoms; (C) ring model, with the $H_2O$ molecules on diagonally opposite Li atoms.

for the twelve bonds in the stack). Furthermore, the Li···Li and N···N contacts are on average longer than those in the stack; the former for a central Li atom are 2.444 Å across the inner ring, 2.341 Å across an outer ring, and 3.780 Å going along the ladder to an outer Li atom (average of all three contacts, 2.855 Å), and the respective values for a central N atom are 3.435, 3.224, and 3.888 Å (average, 3.516 Å). It is also pleasing to note the good agreement between the geometry of this optimized $(LiNH_2)_4$ ladder and the geometries found in the crystal structures of complexes **1** and **2**. For angles, those at Li and N in the planar central ring of $(LiNH_2)_4$, 109.2° and 70.8°, respectively, can be compared with averaged values of 108.2° and 71.8°, respectively, for **1** and **2**. The N–Li distances also lend strong support to our rationalization of how such ladders are assembled by joining rings (Scheme III): thus, the four distances around the central ring (representing N–$Li_2$ 3-center bonds) are indeed all much longer (range, 2.060–2.155 Å; average, 2.108 Å) than those found for the remaining three bonds (two-center ones) exclusive to each outer ring (range, 1.882–1.980 Å; average, 1.942 Å).

The Mulliken charge distribution for all three models of $(LiNH_2)_4$ gives the expected polarization of electron charge away from the Li and H atoms and toward the N atoms, resulting in excess charge of ~1.0 e on all N atoms. For the ladder model, the outer Li atoms are less positively charged (+0.44e) than the three-coordinate Li atoms (+0.63e) of the inner ring. In contrast, the net charges on all the amido groups are similar (inner groups −0.53e, outer ones −0.54e), so that the inner four-membered ring has a net positive charge whereas the outer rungs bear a negative charge. The charges on the Li centers present in the ring and cubane molecules are +0.52e and +0.55e, respectively, and thus are similar in magnitude to the Li charges found within monomeric $LiNH_2$ (+0.58e), the ring dimer $(LiNH_2)_2$ (+0.57e), and the ring trimer $(LiNH_2)_3$ (+0.54e).[4]

We have previously shown, with the help of calculations on model systems, that the presence of Lewis bases coordinated to Li can influence the choice of degree of association of lithium amides between trimerization and dimerization.[4] In the absence of such bases the trimerization process is clearly preferred, while, in their presence, it was surmized that complexed dimers would be the energetically preferred products. For the tetramers of $LiNH_2$, base complexation could, in a similar manner, be a crucial factor in determining the ensuing structure, and so some simple models of solvated ladder and ring structures of $(LiNH_2)_4$ were examined theoretically, using $H_2O$ as the model donor and STO-3G as the basis set; in view of the results described above for uncomplexed $(LiNH_2)_4$ species, stacked structures were not examined further. Initially the base-free tetramers were recalculated at this lower basis set to check whether there was any dramatic alteration in differential energy values and in structural parameters compared to those calculated at the 6-31G level since the STO-3G basis set is known to be subject to basis set superposition error.[5c] For the STO-3G calculations, the ring is found to be more stable than the ladder by 10.9 kcal $mol^{-1}$ (cf. 7.4 kcal $mol^{-1}$ at 6-31G), while, for both these models, it is found that Li–N bond lengths are slightly shorter (by ~0.08 Å) and that angles agree to within 3° when compared to the 6-31G optimized structures. These differences are not too great, and so the lower basis set proves acceptable. Thus it was used to examine ring and ladder models of $(LiNH_2)_4 \cdot 2H_2O$ and $(LiNH_2)_4 \cdot 4H_2O$; the resulting geometries are shown in Figures 8 and 9, while the energies of these species are recorded in Table II.

**Table II.** The Electronic Energies of $(LiNH_2)_4 \cdot nH_2O$ (for $n$ = 0, 2, 4) Calculated at the STO-3G Level

| model | total energy (au) | rel energy (kcal $mol^{-1}$) | coordination energy (kcal $mol^{-1}$) |
|---|---|---|---|
| | (i) $(LiNH_2)_4$ | | |
| ring ($D_{4h}$) | −249.276 66 | 0 | |
| ladder ($C_{2h}$) | −249.259 24 | 10.9 | |
| | (ii) $(LiNH_2)_4 \cdot 2H_2O$[a] | | |
| **A** (ladder) ($C_{2h}$) | −399.326 83 | 0 | 85.2 |
| **B** (ladder) ($C_{2h}$) | −399.315 56 | 7.2 | 67.1 |
| **C** (ring) ($C_{2v}$) | −399.315 56 | 7.2 | 67.1 |
| | (iii) $(LiNH_2)_4 \cdot 4H_2O$[a] | | |
| **D** (ring) ($D_{4h}$) | −549.323 48 | 17.1 | 114.9 |
| **E** (ladder) ($C_{2h}$) | −549.277 46 | 62.9 | 80.0 |
| **F** (ladder) ($C_{2h}$) | −549.350 64 | 0 | 142.9 |

[a] Model notation given in the text and in Figures 8 and 9.

Three models of $(LiNH_2)_4 \cdot 2H_2O$ were examined initially, two being based on the ladder structure with $H_2O$ molecules bound to outer Li atoms (A) and to inner Li atoms (B), and the third model (C) consisting of an eight-membered ring with $H_2O$ molecules coordinated to just two diagonally opposite Li atoms [Figure 8, (A) and (C) optimized structures]. The optimization process on B did not result, for reasons given below, in a third unique structure since the resulting geometry was identical with that of model C. Pleasingly, though, of A and C, structure A is more stable, by 7.2 kcal $mol^{-1}$, i.e., complexation, even by just two base molecules within amides containing four Li centers, has reversed the ring-over-ladder structural preference found for "bare" $(LiNH_2)_4$ species. In fact, both A and C show a marked lowering of energy due to water coordination, 85.2 and 67.1 kcal $mol^{-1}$, respectively, but it is the difference (18.1 kcal $mol^{-1}$) between these coordination energies which has enabled the bis(outer Li-solvated) ladder to become more stable than the ring. These energy changes involving A and C can be correlated with geometry changes, vis à vis STO-3G optimized structures for $(LiNH_2)_4$ as a ladder and as a ring, at the coordination sites. Thus, for the ladder model, the NLiN angles at the outer rungs change little (112.1° to 108.2°) upon coordination, while, for the ring model, the angles at Li need to alter much more markedly (162.4° to 138.4°) to accommodate $H_2O$ ligands. In fact, the nonappearance of an energy minimum associated with model B can also be correlated with required geometrical reorganizations: for B, the Li sites to undergo $H_2O$ coordination are already three-coordinate since they are central ones, and this reorganization to accommodate bis-(complexation) is such that it cleaves the inner Li–N bonds of the ladder.

Three models of $(LiNH_2)_4 \cdot 4H_2O$ were considered, and their optimized structures are shown in Figure 9. Model D was based on the ring tetramer with each Li atom complexed by a single $H_2O$ molecule, and models E and F had ladder arrangements, E with an $H_2O$ ligand attached to each Li atom while F has two $H_2O$ molecules coordinated to each of the two outer Li centers. The most stable of these three structures is F, which is 17.1 and 62.9 kcal $mol^{-1}$ lower in energy than D and E, respectively. Thus the preference for a ladder over a ring structure upon complexation, noted earlier for the $(LiNH_2)_4 \cdot 2H_2O$ species (ladder A then being more stable than ring C by 7.2 kcal $mol^{-1}$), has been confirmed and, indeed, magnified in the case of structures F and D. For the preferred complexed ladder F compared to the complexed ring D, this preference arises because such addition of four $H_2O$ molecules to a ladder results in a gain in stability of 142.9 kcal $mol^{-1}$ while similar addition to a ring lowers the energy by only 114.9 kcal $mol^{-1}$. In turn, these results can be explained by

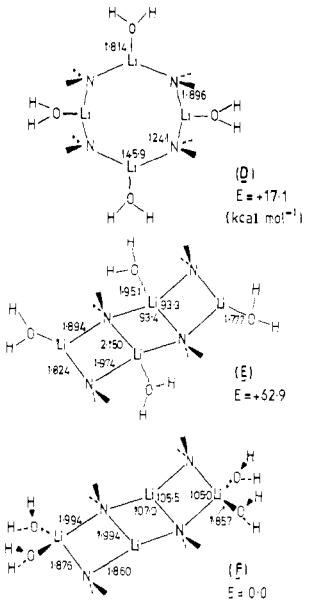


**Figure 9.** Ab initio optimized geometries (STO-3G) of $(LiNH_2)_4 \cdot 4H_2O$: (D) ring model; (E) ladder model with an $H_2O$ attached to each Li; (F) ladder model with two $H_2O$ attached to each outer Li.

considering the degree of reorganization required in each case. Thus the NLiN angles at the outer Li atoms of the ladder model are reduced by just 7° (to 105.0°, Figure 9F) while each NLiN angle of the ring model decreases by 16.5° (to 145.9°, Figure 9D). Comparison of the energies of models E and F with those of the bis(complexed) ladder A plus two free $H_2O$ molecules reveals that the extra coordination of two $H_2O$ at the outer Li atoms results in a gain in stability of 57.7 kcal mol$^{-1}$, while their coordination at the inner Li atoms gives an extra stabilization energy of only 11.8 kcal mol$^{-1}$. This last-noted, relatively low gain reflects the crowded nature of the geometry about the inner Li atoms within a ladder structure; comparing the inner, central ring NLiN angles of $(LiNH_2)_4$ [at STO-3G level] with those of E, then it is seen that in order to accommodate two $H_2O$ molecules at these two Li sites these angles would need to reduce from 108.7°, 102.5° to 93.4°, 93.3°, respectively. The resulting (inner)Li–O coordinate bond distances in E are 1.951 Å, cf. the much shorter (outer)Li–O distances of 1.758, 1.777, and 1.857 Å found in A, E, and F, respectively. Overall, then, these calculations on $(LiNH_2)_4 \cdot 2H_2O$ and $(LiNH_2)_4 \cdot 4H_2O$ species concur with our experimental results found for complexes **1** and **2**: they help explain why, on provision of bi- and tridentate donors to lithium amides, firstly that there can result a switch of structural preference from ring to ladder and secondly that these donors are not incorporated such that there is one per Li center (even though a 1:1 donor:Li ratio is provided, see Experimental Section), but rather that the inner Li atoms resist complexation, this being restricted to metal atoms at the ends of the ladder.

As a final part of this study, we have attempted to pinpoint the solution behaviors of complexes **1** and **2** in hydrocarbons. Our method is to link variable-concentration cryoscopic relative molecular mass (CRMM) measurements with results from $^7$Li NMR spectroscopy, also obtained on variable-concentration solutions and, in some cases, at variable temperatures. Its use on a range of amido- and iminolithium species which gave distinct signals at 25 °C has been described,[9] as has a study on solutions of iminolithium compounds, $(RR'C{=}NLi)_n$ which are hexamers, $n = 6$ (two stacked trimeric rings), in the solid but appear to undergo further stacking (e.g., to a nonamer, $n = 9$) in solution.[27] Similar methods employing colligative properties (cryoscopy, vapor pressure barometry), but with $^{15}$N, $^{13}$C, and $^6$Li NMR spectroscopic studies on isotopically enriched samples, have recently been

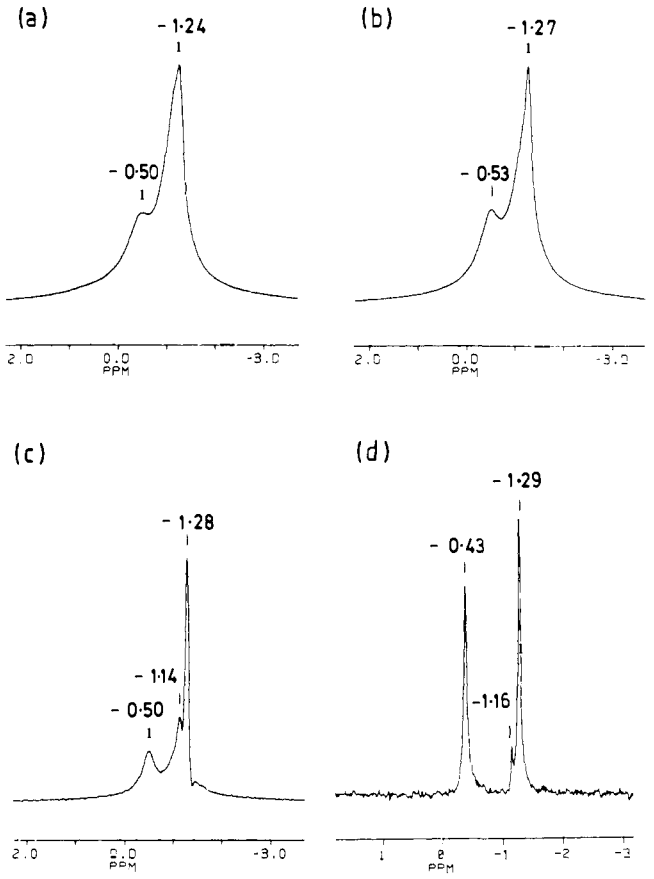


**Figure 10.** Variable-concentration Li NMR spectra of solutions of **2** in $[^2H_8]$toluene at −95 °C: (a) $^7$Li spectrum (139.96 MHz), $5.0 \times 10^{-2}$ mol dm$^{-3}$; (b) $^7$Li spectrum, $2.5 \times 10^{-1}$ mol dm$^{-3}$; (c) resolution enhanced version of spectrum shown in (b); (d) $^6$Li spectrum (52.99 MHz), $6.7 \times 10^{-1}$ mol dm$^{-3}$.

used to investigate the solution equilibria of lithiated cyclohexanone phenylimine complexed by THF[28] and of lithium indolides and anilides in ethers.[29] It is most convenient to discuss first the behavior of complex **2** in hydrocarbon solutions since, in fact, it seems that this dimeric species largely retains its integrity on dissolution. Thus, CRMM measurements on relatively dilute and relatively concentrated solutions of it in benzene ($3.4 \times 10^{-2}$ mol dm$^{-3}$ and $9.0 \times 10^{-2}$ mol dm$^{-3}$, respectively; molarities expressed relative to empirical formula, $n = 1$, of formula mass 270) gave respective RMM values of 546 ± 16 and 568 ± 15, corresponding to respective $n$ values of 2.02 ± 0.06 and 2.10 ± 0.06. Two solutions of **2** in $[^2H_8]$toluene, of concentrations $5.0 \times 10^{-2}$ and $2.5 \times 10^{-1}$ mol dm$^{-3}$, were examined by high field $^7$Li NMR spectroscopy. It is important to stress at this point that a good match cannot always be achieved between the concentrations used in NMR work and those used in cryoscopy: for the latter, the range of concentrations is limited at one end by the need to obtain measurable freezing point depressions and at the other by colligative property laws, while for the former the limits relate, at one end, to obtaining good quality spectra in reasonable acquisition times and, at the other, to solubility. This written, however, it is reasonable to suppose, in view of the CRMM results, that both solutions examined by $^7$Li NMR spectroscopy will contain a preponderance of dimeric **2** with possibly smaller amounts of a higher aggregate (given $n$ values slightly exceeding 2, which may increase somewhat in solutions at low temperatures). Indeed, while both solutions exhibit a sharp singlet at ca. $\delta$ −0.91 ppm in their $^7$Li NMR spectra at 25 °C, their spectra at −95 °C reveal more resonances, as shown in Figure 10. The spectrum of the more

(27) Barr, D.; Snaith, R.; Mulvey, R. E.; Wade, K.; Reed, D. *Magn. Reson. Chem.* **1986**, *24*, 713.

(28) Kallman, N.; Collum, D. B. *J. Am. Chem. Soc.* **1987**, *109*, 7466.
(29) Jackman, L. M.; Scarmoutzos, L. M. *J. Am. Chem. Soc.* **1987**, *109*, 5348.

| Molarity × $10^3$ | $M_r$ | n |
|---|---|---|
| 17 | 699 ± 49 | 1.73 ± 0.09 |
| 20 | 713 ± 33 | 1.77 ± 0.12 |
| 30 | 1356 ± 95 | 3.36 ± 0.24 |
| 49 | 2285 ± 118 | 5.66 ± 0.30 |
| 65 | 2630 ± 122 | 6.51 ± 0.30 |
| 79 | 2164 ± 116 | 5.36 ± 0.29 |
| 88 | 2123 ± 126 | 5.26 ± 0.32 |

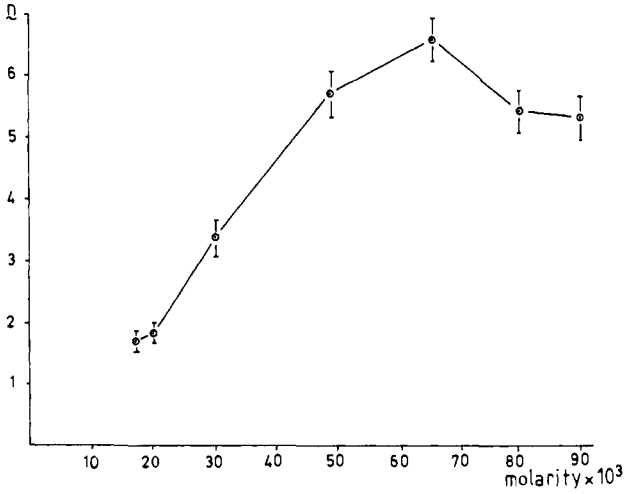


**Figure 11.** Variable-concentration relative molecular mass ($M_r$) and association states (n) found by cryoscopy for **1** in benzene solutions.

dilute solution [Figure 10a] consists of a resonance at $\delta$ −1.24 ppm which is broad and asymmetric, and, to high frequency of this, there is a further, even broader resonance ($\delta$ −0.50 ppm) of lower

**Scheme IV**

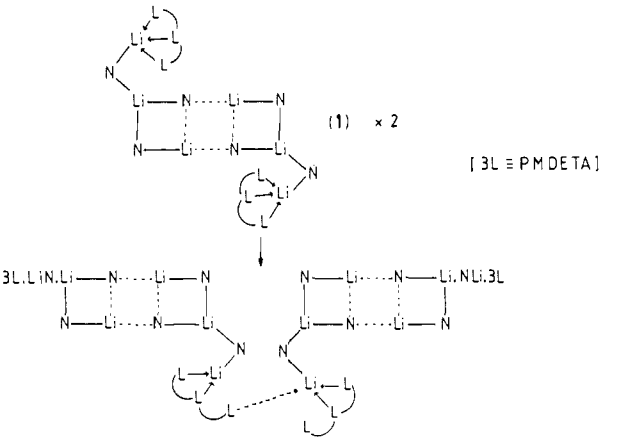


intensity. Very similar features are apparent in the spectrum of the more concentrated solution [Figure 10b], this having the same large resonance ($\delta$ −1.27 ppm) alongside the lower intensity one ($\delta$ −0.53 ppm), though this is now slightly more pronounced. Resolution enhancement of this spectrum [Figure 10c] separates these two signals and also shows that the slight asymmetry observed on the more intense one was due to a third, minor resonance (at $\delta$ −1.14 ppm). Furthermore, the resolution enhanced spectrum also reveals that the two signals at $\delta$ −0.50 and −1.28 ppm seem, in fact, to have approximately equal integrals. To explore this possibility further, we turned to $^6$Li NMR spectroscopy; this nucleus has the major advantage over the $^7$Li one of having a low quadrupole moment and hence will generally give sharper lines. In fact, $^6$Li is primarily relaxed via dipolar relaxation (note the recent use of $^6$Li/$^1$H NOE—often called HOESY experiments[30]).

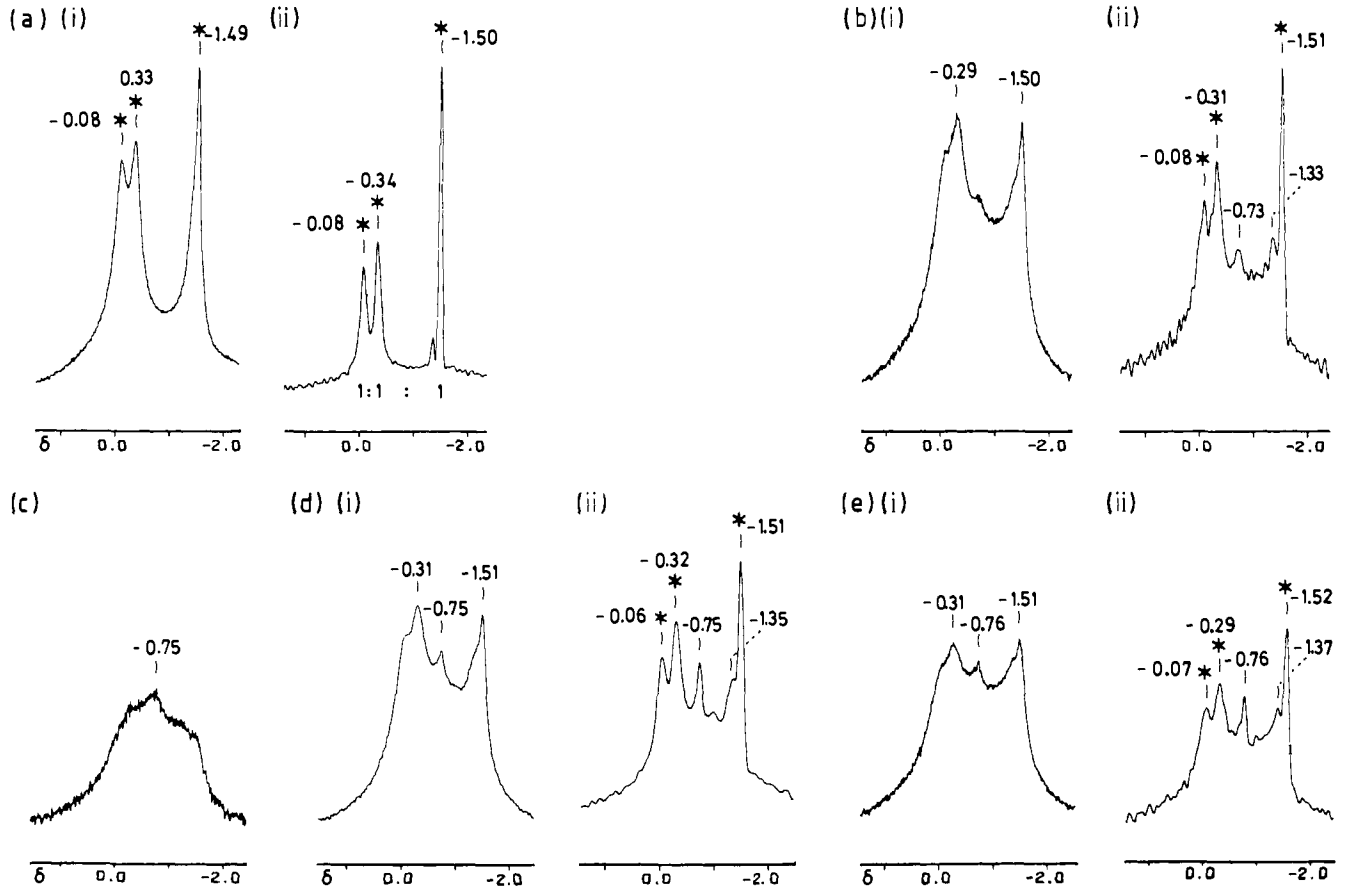


**Figure 12.** Variable-concentration $^7$Li NMR spectra (139.96 MHz) of solutions of **1** in [$^2H_8$]toluene at −95 °C: (a) 0.18 mol dm$^{-3}$, (i) ordinary spectrum, (ii) resolution-enhanced version; (b) 0.09 mol dm$^{-3}$, (i) ordinary spectrum, (ii) resolution-enhanced version; (c) 0.06 mol dm$^{-3}$, ordinary spectrum; (d) 0.035 mol dm$^{-3}$, (i) ordinary spectrum, (ii) resolution-enhanced version; (e) 0.02 mol dm$^{-3}$, (i) ordinary spectrum, (ii) resolution-enhanced version.

The benefit of sharper lines is somewhat counterbalanced by the relative insensitivity of $^6$Li with respect to $^7$Li (natural abundance sensitivities of $^6$Li and $^7$Li with respect to $^{13}$C are 3.6 and ca. 1500, respectively). This fact, combined with the increased interpulse delays needed for $^6$Li, mean that $^6$Li NMR spectra require a greater length of time to acquire and will tend to limit observation to higher concentrations in the absence of isotopic enrichment. Accordingly, we recorded the natural abundance $^6$Li NMR spectrum (52.99 MHz) of a (relatively) very concentrated [$^2H_8$]toluene solution of **2** ($6.7 \times 10^{-1}$ mol dm$^{-3}$) at −95 °C. This [Figure 10d] confirmed that the two signals, as seen via $^7$Li, do indeed possess equal integrals; again, a minor signal was observed at ca. $\delta$ −1.15 ppm.

The fact that the $^7$Li spectra showed no major differences on varying the concentrations of the solutions observed, along with the two major signals being of equal intensities, suggests that these larger signals are given by lithium atoms in the same molecule, presumably the "central" and the "end" lithiums in the dimeric ladder structure. Given the RMM values cited earlier, the minor resonance ($\delta$ ca. −1.1) presumably arises from a higher aggregate of some type.

A more complicated solution behavior pertains for the PMDETA-containing ladder, **1**. Such is apparent on considering CRMM values obtained for solutions of it in benzene (Figure 11; molarities expressed relative to empirical formula $n = 1$, of formula mass 404). At low concentrations, $n$ values slightly below 2 are found, implying that on dissolution dimeric **1** essentially dissolves as such, though it may partially dissociate into a monomer and/or partially lose PMDETA. On increasing the concentration, the association state first also increases, reaching a maximum of $n$ = ca. 6.5, but then begins to fall. One interpretation of these results is that, at relatively low concentrations, PMDETA ligands can partially dissociate in the sense of amending their role from tridentate within each ladder to bi- (or even mono-) dentate. This would initially leave some of the PMDETA-complexed Li centers coordinatively unsaturated (three-, or even two-, coordinate), and it would also leave "free" $Me_2N$ or MeN donor groups. These groups could donate to Li centers in other ladders, i.e., a particular PMDETA ligand might act as bidentate within a particular ladder, its third donor functionality linking to other ladders. In this way (depicted diagramatically in Scheme IV) two, three, or more ladders could join together, to give $n$ values of 4, 6, etc. (Such further association cannot be due to initial partial dissociation of **1** into monomers since these would simply have but one option, to rejoin, i.e., dimer ↔ monomer equilibria would be set up, with $n$ always ≤2; nor can it be due to total *loss* of PMDETA ligands since then $n$ could never exceed 2). However, these dissociative–associative processes are competitive ones, the latter (which relies on the former) being encouraged at higher concentrations but the former at lower ones. More specifically, there must come a (higher) concentration at which PMDETA amendment begins to be suppressed, so that there are fewer coordinatively unsaturated dimeric ladders available for further association: for this reason, $n$ begins to decrease. $^7$Li NMR spectra recorded on solutions of **1** lend general support to these interpretations. A selection of these spectra, all recorded at −95 °C on solutions of widely differing concentrations, is shown in Figure 12. For an extremely concentrated solution (approximately double that of the most concentrated solution looked at by cryoscopy), the spectrum consists of just three signals [Figure 12a, (i) ordinary spectrum, (ii) line-narrowed spectrum] of equal integrals, assignable to the three types of Li atoms in dimeric **1** itself; two of these are close together, with the third quite separate, and so correspond to the two sets of three-coordinate Li atoms within the ladder and to the four-coordinate, PMDETA-complexed Li atoms, respectively. At this high concentration, then, partial PMDETA dissociation has been completely suppressed, resulting in the presence of dimeric **1** alone in solution. Two-fold dilution (to give a solution of about the same concentration as that giving $n = 5.26$ by cryoscopy) gives a solution whose $^7$Li NMR spectrum is much more complicated [Figure 12b]: the three signals (asterisked) attributed to intact **1** are still apparent, along with smaller distinct resonances at $\delta$ −0.73 and −1.33 ppm and probably many more underneath these peaks. This complexity increases on further dilution, giving the spectrum shown in Figure 12c [roughly corresponding in concentration to the solution which gave the maximum $n$ value, ca. 6.5] which consists of just one broad, ill-defined mass of resonances; crucially, though, for yet more dilute solutions, the spectra begin to simplify again, and distinct signals due to the dimer re-emerge [Figure 12d and e]. These solutions are of sufficient dilution to allow partial PMDETA dissociation/amendment but then to allow only limited association of the partially "bare" ladders which result. Further NMR experiments, particularly ones involving $^6$Li, $^{15}$N nuclei, are in progress, in the hope of further confirming and clarifying these complex solution equilibria.

**Acknowledgment.** We thank the S.E.R.C. (D.B., W.C., S.M.H., R.S.) and the Royal Society (R.E.M.) for financial support, the S.E.R.C. for provision of high field NMR facilities, and Professor P. v. R. Schleyer and Dr. W. Bauer for useful discussions.

**Registry No. 1**, 105560-24-5; **2**, 120771-53-1; $H_2\overline{C(CH_2)_3}NLi$, 4439-90-1; Bu-*n*-Li, 109-72-8; $(LiNH_2)_4$, 98331-83-0; $(LiNH_2)_4 \cdot 2H_2O$, 120771-54-2; $(LiNH_2)_4 \cdot 4H_2O$, 120771-55-3.

**Supplementary Material Available:** Tables of atom coordinates, anisotropic thermal parameters, and bond distances and angles (8 pages); tables of observed and calculated structure factors with standard deviations (31 pages). Ordering information is given on any current masthead page.

(30) Bauer, W.; Clark, T.; Schleyer, P. v. R. *J. Am. Chem. Soc.* **1987**, *109*, 970.